Effect of intralayer inhomogeneity on helical superstructures of liquid crystals

W. Jeżewski*

Institute of Molecular Physics, Polish Academy of Sciences, Smoluchowskiego 17, 60-179 Poznań, Poland

(Received 24 February 2012; published 29 May 2012)

A mechanism to form distorted helical structures in ferroelectric liquid crystals is presented. It is shown that the deformation of helical interlayer structures of thin smectic systems can be considered as a direct consequence of the surface-induced spatial inhomogeneity in the distribution of the azimuthal molecular orientation within smectic layers. The intralayer azimuthal nonuniformity occurring in helical phases is argued to generate a local depolarizing electric field of the strength varying not only in smectic layers but also between the layers. The resulting modulation of the depolarization level in the direction of helical axes is shown to lead to a distortion of helices. Using a simple model, including the depolarization interaction, it is demonstrated that the degree of the helix deformation strongly varies as parameters of the model are changed. It is also shown that strong deformations of extremely short helices, found for appropriate values of the parameters, reflect nonuniformity of helicoidal superstructures of respective smectic subphases in real liquid crystalline systems.

DOI: 10.1103/PhysRevE.85.051702 PACS number(s): 61.30.Gd, 61.30.Eb, 77.80.−e

I. INTRODUCTION

The understanding of a large polymorphism of helical ferroelectric liquid-crystal (LC) systems still remains one of the most challenging problems in researches of the molecular order of liquid crystals, a field of great importance in modern display technologies. Investigations of helicoidal polar ordering of smectic LCs have been stimulated by the discovery of the helical antiferroelectric phase Sm C_A^* and then by detecting other smectic subphases, especially by identifying the antiferroelectric subphase Sm C_β^* and the ferrielectric subphase Sm C_γ^*, displaying deformed three- and four-layer helicoidal structures, respectively. Perhaps the most intriguing subphase, undoubtedly detected, is the ferroelectric Sm C_α^* phase, having a regular (undeformed) structure with a short helical period, typically, close to six smectic layers [1]. It has experimentally been shown that the pitch in this subphase can evolve across a few smectic layers upon cooling, reaching the value even less than three layers (but greater than two layers) [2]. Generally, periods of helical structures of the variant subphases are incommensurate (with the thickness of smectic layers), although a distorted molecular smectic structure with the commensurate six-layer periodicity has recently been identified in freestanding LC film systems [3].

To explain the formation of complex structures of the smectic subphases, the stability of these subphases, and sequences of phase transitions between them, various phenomenological (by necessity) models have been developed. These models usually involve a local (in-layer) two-dimensional order parameter characterizing the orientation of the molecular director and, in general, a polar order parameter determined by the spontaneous polarization of a smectic layer [4–13]. In simplified models, the molecular orientation within a given smectic layer is characterized solely by the azimuthal angle [14–17]. In order to formulate a unified model that would be valid for a wide range of helical periods, not only for long periods but also for extremely short periods (typical, e.g., for the Sm C_α^* phase) as well as for multilayer helical structures, the space variable in the direction perpendicular to smectic layers has been treated as a discrete quantity. Then, the free energy of helical smectic LCs has been determined, in its most basic form, taking into consideration, in addition to usual one-point Landau terms, the piezoelectric (one-point) term, and two-point components corresponding to interactions between molecules belonging to nearest neighbor (NN) and next nearest neighbor (NNN) smectic layers [1], as well as two-point contributions corresponding to couplings of even more distant molecules [11,15]. The NN couplings reflect dipol-dipol, steric, and van der Waals interactions (comprising a possible chiral contribution), while the NNN component reflects the flexoelectric effect [7,10], but also the dipol-dipol coupling [15]. In contrast to the continuous models, which anticipate the existence of only Sm C^* and Sm C_A^* phases, the discrete models additionally predict the appearance of other subphases. Nevertheless, the discrete models suffer a serious drawback since, to reproduce the nonmonotonic temperature dependence of the helical period, experimentally observed in various subphases, couplings inherent in these models should also depend nonmonotonically on temperature.

An essential assumption commonly used to describe helical LCs is that the bulk of LCs can be considered unaffected by cell surfaces or interfaces confining LC substances. Then, helical superstructures of smectic LCs can be modeled in one dimension only, i.e., along the helical axis. However, this assumption cannot be accepted in cases of LCs sandwiched between plates of rather thin cells [18–20], i.e., when surface anchoring interactions induce nonuniform distribution of the molecular azimuthal angle in the direction normal to the sample surfaces. Another mechanism of nonuniform orientation of molecules emerges in freestanding LC film systems [21]. As has been demonstrated, LC-air interfaces occurring in such systems affect orientational states of molecules on relatively large distances from the interfacial surfaces [22]. In this paper, the influence of the space nonuniformity of the azimuthal orientation of molecules on the formation of helical superstructures in ferroelectric chiral LCs with well-defined smectic layers being perpendicular to plates confining cells is investigated.

*jezewski@ifmpan.poznan.pl

II. MODEL

The model considered in this paper concerns an idealized geometry of LC systems with well-defined smectic layers oriented perpendicular to cell plates bounding the LC material. Due to the occurrence of surface anchoring interactions, the orientational states of molecules are not uniform within each of the smectic layers and, consequently, the azimuthal molecular angle ϕ can then be assumed to vary continuously in the direction, say, the x direction, normal to cell plates [19,20]. However, in the y direction, parallel both to cell surfaces and smectic layers, no variation of ϕ is assumed. A possible variability of ϕ, associated with the appearance of helices in the z direction, normal to smectic layers, is described in a discrete way. Hence, the orientation of a molecule located in the ith smectic layer at the distance x from the bottom plate of a cell of thickness d (i.e., at $0 \leqslant x \leqslant d$) is determined by the function $\phi = \phi_i(x)$ with $i = 1,2,\ldots,N$, where N is the number of smectic layers forming the system. (The basic geometry of the studied system is schematically illustrated in Fig. 1.) As a result of nonuniformity of molecular orientations inside smectic layers, there appear local polarization charges that generate local electric fields. Naturally, such induced internal fields interact with electrical dipolar moments of molecules yielding a depolarization contribution to the energy of LC systems [23–25]. Consequently, to study the effect of nonuniformity of the azimuthal molecular angle within smectic layers on the helical structure of chiral smectics, the straightforward (undistorted) clock model [1,26] is extended below to include the depolarization self-interaction. Since surface interactions promote, in general, some special orientations of molecules, these interactions can affect the formation and stability of possible helix superstructures. However, such surface-induced effects are not investigated here. For simplicity, the difference $\phi_{i+1}(x) - \phi_i(x)$, $i = 1,2,\ldots,N$, between azimuthal angles of molecules placed in a neighboring smectic layer, is assumed to be independent of x (though it may not necessarily be true for real systems). Accordingly, $\phi_i(x)$ can be expressed as

$$\phi_i(x) = \phi(x) + \phi_i, \quad i = 1,2,\ldots,N, \tag{1}$$

with $\phi(x)$ being identical for all smectic layers and ϕ_i being independent of x. In order to formulate a unified description of various helical phases, complex n-layer helical structures

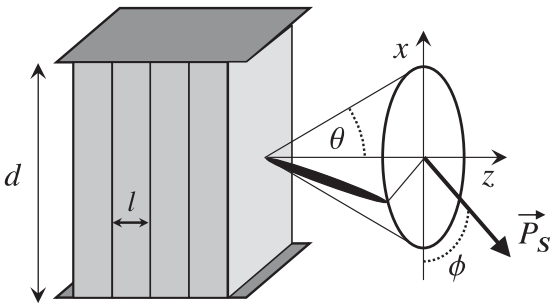

FIG. 1. Assumed simple cell structure with smectic layers being aligned perpendicular to boundary plates of a cell of thickness d. Smectic layer width l, vector of local polarization $\vec{P}_S$, molecular tilt angle θ, and molecular azimuthal angle ϕ are also shown.

($n = 2,3,\ldots$) will be treated here as single (one-layer) helical structures with the period $p = n$, in cases of commensurate (with the smectic layer width) helices, or with the period $p \approx n$ in cases of incommensurate helices. Hence, $p \approx 2,3,4$ in Sm C^*_A, Sm C^*_γ, Sm C^*_β subphases, respectively, and $p \approx 6$ in typical Sm C^*_α subphase. Accordingly, p is defined here as the pitch length $\bar{p}$ expressed in the unit of the smectic layer width l, i.e., $p = \bar{p}/l$.

The resulting free energy of a tilted chiral smectic phase exhibiting a helical superstructure is then determined by

$$F = \frac{1}{2}\sum_{i=1}^{N}\int_0^d \left\{K_x[\partial_x\phi(x)]^2 + K_z l^{-2}(\delta_i - q_0)^2 + \frac{P_S^2}{\varepsilon_0}\cos^2\phi_i(x)\right\} dx, \tag{2}$$

where K_x and K_z are the intralayer and interlayer elastic constants, respectively, l denotes the smectic layer width, $q_0 = 2\pi/p_0$, with p_0 being the period of an undeformed helix, P_S is the local polarization, and

$$\delta_i = \phi_{i+1} - \phi_i. \tag{3}$$

The first two components in Eq. (2) represent the intralayer and interlayer elastic energy, respectively, while the last term describes the depolarization energy [23–25]. It should be pointed out that both the elastic constants K_x and K_z contain the factor $\sin^2\theta$, where θ is the molecular tilt angle. Clearly, the difference δ_i between azimuthal angles of molecules placed in adjacent smectic layers is identical for all i, i.e., $\delta_i \equiv q_0$ for all i, within the undistorted clock model, but, as will be shown, can vary between successive pairs of layers when the depolarization effect is taken into account. Note that q_0 is related to the helical wave number and characterizes the molecular twist from one layer to the next layer, originating, e.g., in the chiral structure of molecules.

Inserting Eq. (1) into Eq. (2), one can separate the intra- and interlayer contributions to the free energy. One must, however, proceed with caution. Indeed, in the expression for F, there arises a "mixed" term of the type $\int_0^d \sin 2\phi(x)\,dx \sum_{i=1}^N \sin 2\phi_i$ which is, in general, nonzero. Obviously, the sum in this term is equal to zero in cases of undistorted commensurate helices and is close to zero in cases of undistorted and distorted incommensurate helices, provided that $N \gg p$. Thus, in such cases, the mixed contribution to F is equal to zero, or is negligibly small (in absolute value). Moreover, one can infer that, owing to the form of the dependence of depolarization interaction on the azimuthal molecular angle, the relation $\sum_{i=1}^N \sin 2\phi_i = 0$ is also satisfied in the case of distorted commensurate helices allowed within the studied model. Consequently, the mixed term can be omitted, and then one has

$$F = N f_0 + d\, f_h, \tag{4}$$

where

$$f_0 = \frac{1}{2}\int_0^d \left\{K_x[\partial_x\phi(x)]^2 + \frac{P_S^2}{\varepsilon_0}\sin^2\phi(x)\right\} dx \tag{5}$$

corresponds to the intralayer part of the free energy, and

$$f_h = \frac{1}{2}\sum_{i=1}^{N}\left[K_z l^{-2}(\delta_i - q_0)^2 + \frac{c P_S^2}{\varepsilon_0 d}\cos^2\phi_i\right] \quad (6)$$

refers to the free energy contribution associated with the helix formation. The second component of Eq. (6) comes from the surface-induced depolarization. This component of f_h can be interpreted as a sum of fundamental depolarization energy levels of successive smectic layers. The coefficient c is determined by

$$c = \int_0^d \cos[2\phi(x)]dx. \quad (7)$$

It must be stressed that the depolarization contribution to the free energy F does not contain a balancing component that corresponds to uniform distribution of the molecular azimuthal angle within smectic layers and that compensates the depolarization term [the third term in Eq. (2)] when $\phi_i(x), i = 1,2,\ldots,$ becomes independent of x. Consequently, Eq. (2), and thereby Eqs. (5) and (6), are justified only if the azimuthal angle is nonuniformly distributed in each of the smectic layers. Thus, the coefficient c cannot be considered as a depolarization strength, which tends to zero in the limit of uniform distribution of the azimuthal angle. Clearly, c can be equal to zero even if the molecular azimuthal angle depends on x. It follows from Eq. (7) that the coefficient c can essentially take values from the range $[-d,d]$, but to calculate this coefficient, a knowledge of surface-anchoring interactions would be required [20]. Using Eqs. (4)–(7), one can easily check that, if any helices do not appear, i.e., if $q_0 = 0$ and $\phi_i \equiv 0, i = 1,2,\ldots,N$, the formula for the free energy F reduces to

$$F = \frac{1}{2}\int_0^d \left\{K_x[\partial_x\phi(x)]^2 + \frac{P_S^2}{\varepsilon_0}\cos^2\phi(x)\right\}dx, \quad (8)$$

as it should be [24,25]. Minimizing the functional F [Eqs. (4)–(6)] with respect to ϕ_i, one gets the following iterative equation

$$\delta_{i+1} = \delta_i - b\sin 2\phi_i, \quad i = 1,2,\ldots, \quad (9)$$

where $\phi_i = \Sigma_{j=1}^{i}\delta_j$ and the nonlinearity parameter b is given by

$$b = \frac{c\,l^2 P_S^2}{2\varepsilon_0 K_z d}. \quad (10)$$

It is seen that Eq. (9) does not involve q_0. However, to solve this equation, one has to choose appropriate initial values both for δ_1 and ϕ_1 (in addition to a respective value of the parameter b). It is natural to assume that $\delta_1 = q_0$, while ϕ_1 can be treated as a free parameter or can be adjusted to minimize the reduced component $\bar{f}_h = 2l^2 f_h/(NK_z)$ of the free energy part. This reduced contribution to the free energy, given by the relation

$$\bar{f}_h = N^{-1}\sum_{i=1}^{N}[(\delta_i - q_0)^2 + 2b\cos^2\phi_i], \quad (11)$$

contains only one (dimensionless) coupling parameter b.

III. RESULTS AND DISCUSSION

The model is explored below for a value of material parameter b being typical for Sm C^* phases. Taking $l = 2\times10^{-9}$ m, $P_S = 10^{-5}$ Cm^{-2}, $K_z = 10^{-13}$ N, and assuming that $c = 0.5\,d$, one obtains $b = 1.1\times10^{-4}$. This value of the parameter has been used to derive most of the results presented in this section, but greater values of b have also been adopted. Clearly, even if b is small, there can appear *transitory* fluctuations in corresponding sequences of ϕ_i, determined modulo 2π, for initial iterations of Eq. (9), starting with arbitrarily chosen values of ϕ_1 and δ_1. Such transitory effects have been eliminated here by neglecting long initial sequences of ϕ_i, where $i = 1,2,\ldots,N_0$ with $N_0 \gg 1$. Next, subsequent sequences $\phi_{N_0+1},\phi_{N_0+2},\ldots,\phi_{N_0+N_1}$ with $N_1 \gg 1$ have been registered.

The variability of ϕ_i determined by using Eq. (9) is shown in Fig. 2 for $\phi_1 = 0$ and for two different values of $\delta_1 = 2\pi/p_0$, related to $p_0 = 100$ and $p_0 = 400$. This figure illustrates a general rule that the distribution of the molecular azimuthal angle along the helix axis is uniform or, more exactly, approximately uniform when δ_1 is sufficiently small and becomes increasingly nonuniform when δ_1 decreases, provided that ϕ_1 remains unchanged. Moreover, the period p of a distorted helix differs from p_0 in a way that the resulting absolute difference $|p - p_0|$ increases when p_0 grows (at fixed ϕ_1), as demonstrated in Fig. 3 for p being rounded down to nearest integers. The period p has been represented here by integers in order to better visualize its dependence on large values of δ_1, for which p exhibits very large relative fluctuations. Note that δ_1 has been taken very densely in the range of large values, and the function shown in Fig. 3 is single-valued. It should be pointed out that a growing

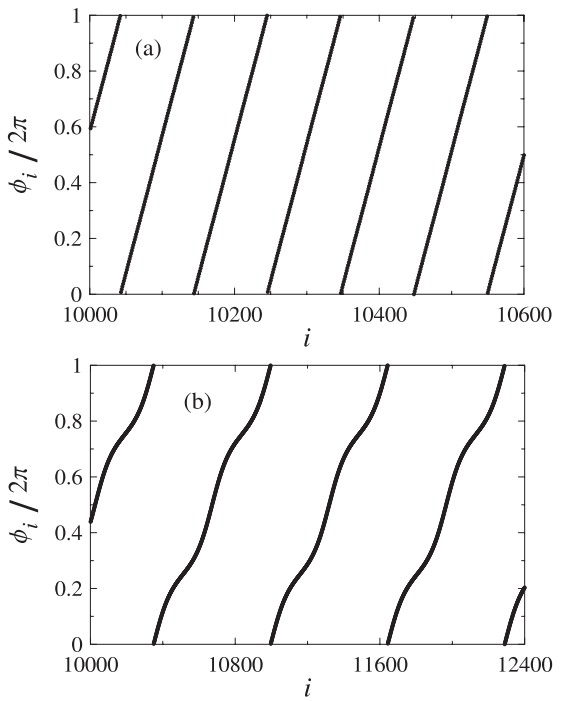

FIG. 2. Distribution of the azimuthal angle plotted modulo 2π for $b = 1.1\times10^{-4}$, $\phi_1 = 0$, $p_0 = 100$ (a), and $p_0 = 400$ (b).

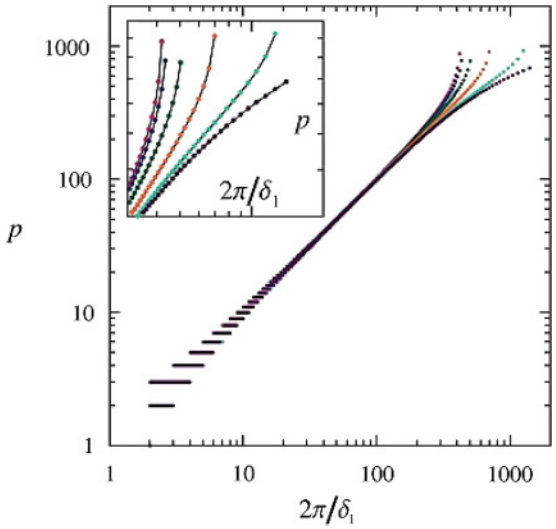

FIG. 3. (Color online) Dependence of the helix period p (approximated by nearest integers) on $p_0 = 2\pi/\delta_1$ drawn for $b = 1.1 \times 10^{-4}$ and for $\phi_1 = 0, 0.1, 0.2, 0.3, 0.4, 0.5$, from left to right. The inset shows a magnified view of the graph fragment obtained for $p_0 \geqslant 300$.

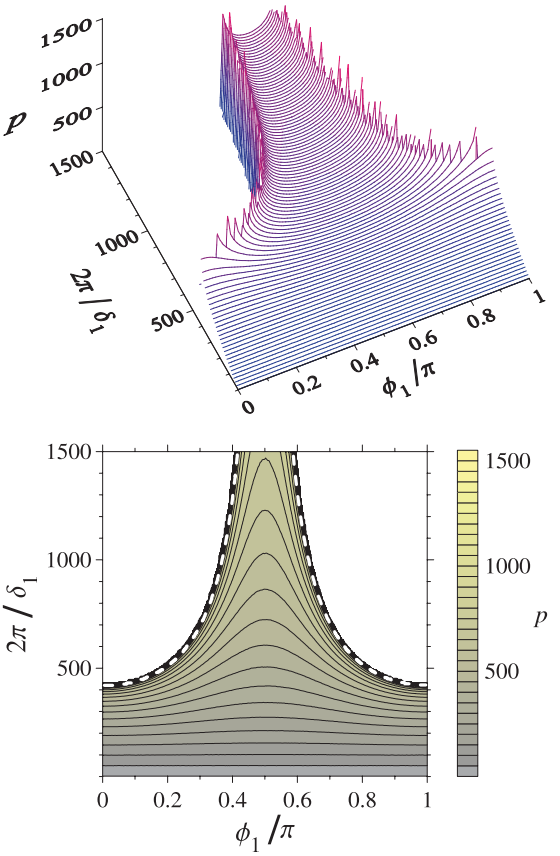

FIG. 4. (Color online) Dependence of the helix period p on $p_0 = 2\pi/\delta_1$ and ϕ_1, as determined for $b = 1.1 \times 10^{-4}$ and $N_0 = N_1 = 10^6$. The lower diagram shows the respective contour map, where the dashed lines represent the critical function $p^{(c)}(\phi_1)$ (see the text). The region of the map associated with $p_0 = 2\pi/\delta_1 > p^{(c)}(\phi_1)$ refers to initial values of δ_1 and ϕ_1 for which sequences of ϕ_i have not any helicoidal character.

deviation of p from p_0 is associated with increasing distortion of respective helices. Similar to p, this deviation is determined not only by δ_1 but also by ϕ_1 (see Fig. 3). It is remarkable that the helix period p can take only finite values, as shown in Fig. 4 for typical values of the helical period $2 \leqslant p_0 \leqslant 1500$. More precisely, there exists a critical line $p_0 = p^{(c)}(\phi_1)$ (represented by the dashed line in the bottom diagram of Fig. 4) that separates the plane of initial values of δ_1 and ϕ_1 into subsets for which ϕ_i [generated by the iterative relation Eq. (9)] exhibits different asymptotic behaviors. It proves that $p^{(c)}(\phi_1)$ is finite for all ϕ_1 and that the studied model does not predict the appearance of any helix when $p_0 > p^{(c)}(\phi_1)$. It should be noted, however, that a detailed analysis of the asymptotic properties of ϕ_i as $i \to \infty$ becomes difficult to carry out for p_0 close to $p^{(c)}(\phi_1)$ and for $\phi_1 \approx \pi/2$, due to long transitory effects. As shown in Fig. 4, the disappearance of helices as $p_0 \nearrow p^{(c)}(\phi_1)$ at a given ϕ_1 is not connected with an infinite elongation of p. When p_0 exceeds $p^{(c)}(\phi_1)$, the molecular azimuthal angle displays, in general, oscillations along the normal to smectic layers. The amplitude of these oscillations is less than 2π and rapidly decreases as p_0 grows. Consequently, one can conclude that the self-depolarizing interaction, leading to the nonuniformity of the distribution of the azimuthal angle along the helix axis, influences the helix period and even imposes an upper limit on the helical period.

To investigate how the depolarizing interaction affects the stability of the studied model system, the reduced free energy contribution $\bar{f}_h$ due to the helix formation has been calculated for various values of δ_1 and ϕ_1. The resulting dependence of $\bar{f}_h$ is presented in Fig. 5. A simple comparison of plots of Figs. 4 and 5 reveals that the disappearance of helices as δ_1 and/or ϕ_1 are appropriately varied is accompanied with a relatively large increase of $\bar{f}_h$. It is important to note that $\bar{f}_h$ rapidly changes as $p_0 \searrow 2$ (see the top diagram of Fig. 5). For $p_0 = 2$ and, in consequence, for $p \approx 2$, $\bar{f}_h$ reaches an absolute minimum as ϕ_1 tends to $\pi/2$. Thus, at this special value of ϕ_1, the resulting Sm C_A^* phase is the most stable of all possible helicoidal phases predicted by the studied model.

It follows from Eq. (11) that the deformation of the helix is associated with an increase of the interlayer elastic part $\bar{f}_{he} = N^{-1} \sum_{i=1}^{N} (\delta_i - q_0)^2$ of the reduced free energy $\bar{f}_h$ and, simultaneously, is connected with a respective change of the depolarization part $\bar{f}_{hd} = 2bN^{-1} \sum_{i=1}^{N} \cos^2 \phi_i$. Clearly, $\bar{f}_{he}$ is greater than zero not only when the system exhibits any distorted helical superstructure but also when any helical superstructure does not appear. Thus, $\bar{f}_{he}$ can be considered as a measure of the nonuniformity of distribution of azimuthal angle of molecules in successive smectic layers only if the system forms a helix superstructure. As concerns $\bar{f}_{hd}$, the influence of the nonuniformity of the molecular azimuthal orientation on this part of the reduced free energy appears to be more complex than in the case of $\bar{f}_{he}$. One can expect, however, that $\bar{f}_{hd}$ decreases as p_0 tends to $p^{(c)}(\phi_1)$, both as $p_0 \nearrow p^{(c)}(\phi_1)$ and as $p_0 \searrow p^{(c)}(\phi_1)$. The result of the interplay between modifications of these two contributions to $\bar{f}_h$ due the helix distortion is graphically presented in Fig. 6 for $p_0 = 2, 6, 500$, and for varying ϕ_1. It is seen that, in the special case of $p_0 = 2$, the depolarization part of $\bar{f}_h$ displays, in contrast to $\bar{f}_{he}$, a relatively rapid increase as $\phi_1 \to 0$ and as $\phi_1 \to \pi$.

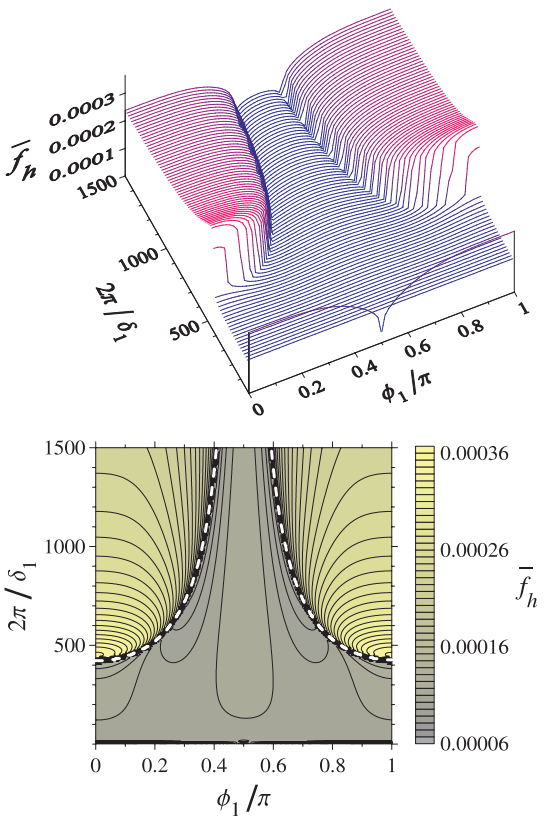

FIG. 5. (Color online) Dependence of the reduced free energy part $\bar{f}_h$, associated with the helix formation, on ϕ_1 and δ_1, as determined for $b = 1.1 \times 10^{-4}$ and $N_0 = N_1 = 10^6$. The lower graph shows the corresponding contour map. The dashed lines on this map represent the critical function $p^{(c)}(\phi_1)$.

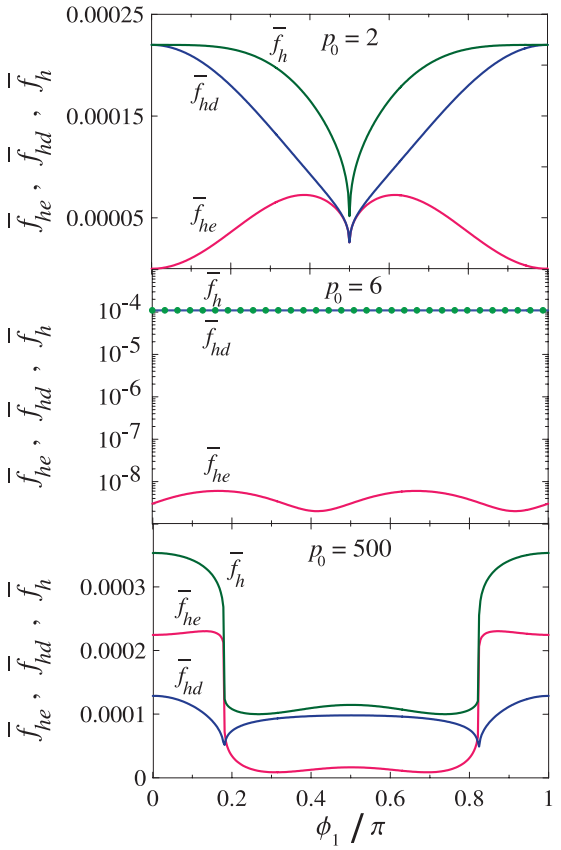

FIG. 6. (Color online) Dependence of $\bar{f}_{he}$, $\bar{f}_{hd}$, and $\bar{f}_h = \bar{f}_{he} + \bar{f}_{hd}$ on ϕ_1, obtained for $p_0 = 2, 6, 500$ (from top to bottom). The dotted line in the middle diagram of the figure corresponds to $\bar{f}_h$. All plots have been drawn using the data of Fig. 5.

In consequence, the corresponding orientational states of molecules become energetically unfavorable. Nevertheless, $\bar{f}_{he}$, $\bar{f}_{hd}$, and, thereby, $\bar{f}_h$ all possess a minimum at the point $\phi_1 = \pi/2$. However, the minima of $\bar{f}_{hd}$ and $\bar{f}_h$ have a global character, while the respective minimum of $\bar{f}_{he}$ is only local. As already discussed, possible helices appearing for p_0 being much less than $p^{(c)}(\phi_1)$ are nearly undistorted. Then, $\bar{f}_{hd} \gg \bar{f}_{he}$ and both the parts of $\bar{f}_h$ are slowly varying functions of ϕ_1, as illustrated in the middle diagram of Fig. 6 for $p_0 = 6$. It is rather surprising that the dependence of $\bar{f}_{he}$ on ϕ_1 determined for $p_0 = 6$ is not symmetric with respect to $\phi_1 = \pi/2$. In cases of helices found for $p_0 > p^{(c)}(\phi_1)$, the functions $\bar{f}_{he}$, $\bar{f}_{hd}$, and $\bar{f}_h$ all have, in general, two symmetric minima (with respect to $\phi_1 = \pi/2$), but located at different pairs of values of ϕ_1, as demonstrated in Fig. 6 for $p_0 = 500$. Accordingly, the depolarization interaction strongly affects the dependence of $\bar{f}_h$ on ϕ_1, leading even to a change of positions of minima of $\bar{f}_h$, determined for sufficiently large p_0.

In order to analyze the behavior of the reduced free energy when δ_1 changes, $\bar{f}_h$ has been determined as a function of p_0 for several values of ϕ_1, as shown in Fig. 7. The inset plotted inside this figure concerns the region of $p_0 \ll p^{(c)}(\phi_1)$, for which $p \approx p_0$. It follows from the figure that the dependence of $\bar{f}_h$ on p_0 strongly changes its character as ϕ_1 varies. This is distinctly visible in cases of $\phi_1/\pi = 0, 0.2, 0.4$. For $\phi_1 = 0$, $\bar{f}_h$ has a shallow minimum at a very small value of p_0. In the case of $\phi_1/\pi = 0.4$, $\bar{f}_h$ also possesses a minimum within the region of small values of p_0, such that $p_0 \ll p^{(c)}(2\pi/5)$, but this minimum displays only a local character. Note that a pertinent global minimum of $\bar{f}_h$ occurs at $p_0 = p^{(c)}(2\pi/5)$. In contrast, $\bar{f}_h$, determined for $\phi_1/\pi = 0.2$, exhibits, within a region of relatively small values of p_0, an existence of a maximum rather

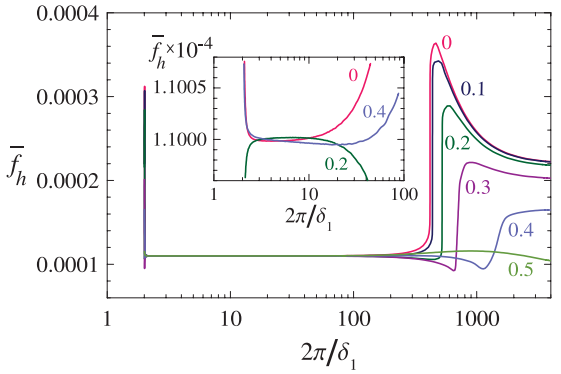

FIG. 7. (Color online) The reduced free energy as function of $p_0 = 2\pi/\delta_1$ for $\phi_1/\pi = 0, 0.1, 0.2, 0.3, 0.4, 0.5$, determined on the basis of the data of Fig. 5. The inset shows a magnification of the diagram, in which typical behaviors of $\bar{f}_h$ are presented for $2 \leqslant p_0 \leqslant 100$. The curves shown both in the main diagram and in the inset are marked with respective values of ϕ_1/π.

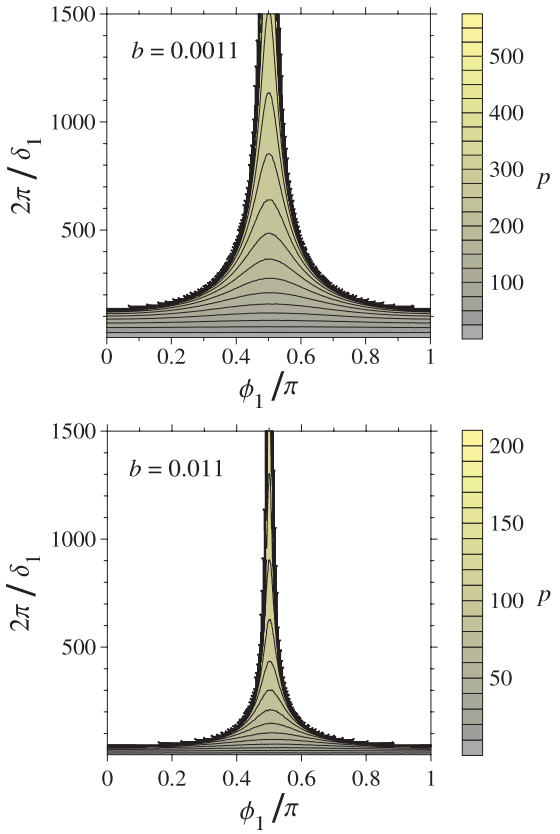

FIG. 8. (Color online) Contour diagrams showing the dependence of the helix period p on $p_0 = 2\pi/\delta_1$ and ϕ_1, determined for $N_0 = N_1 = 10^6$ and, respectively, for $b = 0.0011$ and $b = 0.011$. Blank regions of the diagrams are associated with values of δ_1 and ϕ_1 for which any helix does not appear.

than any minimum. Indeed, the only minimum that $\bar{f}_h$ reveals for $\phi_1/\pi = 0.2$ is located at $p_0 = p^{(c)}(\pi/5)$. Consequently, the model under considerations permits the occurrence extremely short-period helix structures, which are stable with respect to deviations of ϕ_1 from its special values.

It is clear that the function $p_0 = p^{(c)}(\phi_1)$ depends on the material parameter b. Since the parameters K_z and P_S can rapidly vary as temperature is changed, also the parameter b can considerably vary with temperature [see Eq. (10)]. This is the case, e.g., when temperature tends to the critical value, at which the Sm C^*- Sm A^* or Sm C^*_A- Sm A^* phase transitions take place [27,28]. To investigate the influence of the variation of the parameter b on the helical structure, the helix period p has been determined as a function of p_0 and ϕ_1 for $b = 0.0011$ an $b = 0.011$. Resulting contour maps are shown in Fig. 8. These maps, together with the contour diagram of Fig. 4, evidently demonstrate that, at any fixed ϕ_1, the maximum value of $p_0 = p^{(c)}(\phi_1)$ at which a helix can exist and, hence, also the maximal helix period p rather rapidly decrease as b grows. Indeed, when $\phi_1 = 0$, one finds that the maximal value of the helix period p is equal to 988 (for $b = 0.000\,11$), 227 (for $b = 0.0011$), 61 (for $b = 0.011$), and 11 (for $b = 0.11$). On the basis of the above discussion, it is obvious that, for large values of the parameter b, the considered model admits the occurrence of both regular (or, more precisely, nearly undistorted) and distorted stable helices of short periods, although distorted helix structures of extremely short periods can arise only if the parameter b is sufficiently large. Consequently, the model yields a simplified description of helicoidal smectic superstructures, which are encountered in various helical subphases, including the newly discovered smectic phase exhibiting a strongly distorted helical structure with six-layer periodicity [3].

As follows from Eq. (10), the parameter b is inversely proportional to the sample thickness d. This suggests that helical structures with larger periodicity are preferred in LC samples of larger thickness (associated with smaller values of b). In fact, such a size effect has experimentally been found by measuring the helical pitch of the same liquid crystalline material, but confined in cells of different thickness [29,30]. It should be pointed out that the dependence of the helical period on the sample thickness is an evident sign of a large role of the surface interactions and, thereby, the intrasmectic layer inhomogeneity of molecular orientations in forming and stabilizing helical superstructures in smectic LCs.

It is also worth noting that local dielectric and/or magnetic anisotropy contributions to the free energy (when constant electric and/or magnetic field are applied to LC cells) display the same functional dependence on the molecular azimuthal angle as the local depolarization energy [31]. Thus, the effect of the distortion of helical superstructures, similar to that induced by depolarization interactions, can also be expected when constant electric and/or magnetic fields are present. However, depending on the sign of electric and magnetic anisotropies, electric and magnetic fields can enhance or suppress the helix distortion caused by depolarization interactions.

Finally, the physical meaning of ϕ_1, i.e., the initial azimuthal angle value needed to solve Eq. (9), should be explained. In contrast to the second initial value parameter, δ_1, the initial azimuthal angle ϕ_1 has been treated here as an arbitrary parameter, which does not have any direct connection to a definite helical structure. However, in consequence of the symmetry breaking character of the depolarization interaction (incorporated in the considered model), the resulting free energy of a given system distinctly depends on ϕ_1, even when any helical superstructure does not appear. Essentially, one would assume that a "proper" value of ϕ_1 is the one at which the reduced free energy $\bar{f}_h$ reaches a minimum (for a given δ_1). It should be stressed, however, that the discussed model does not explicitly involve the surface interactions. These interactions can yield a significant contribution to the free energy of thin LC systems [18], and then the proper value of ϕ_1 would be that value for which the total free energy (containing the surface anchoring contribution) possesses a minimum. Obviously, an extension of the model to include the surface anchoring interactions would require the knowledge of additional parameters, being rather difficult to determine.

IV. CONCLUDING REMARKS

The results presented in this paper show that the surface-induced inhomogeneity of the space distribution of azimuthal orientations of molecules within smectic layers are of great relevance for the formation and stabilization of helical superstructures with very different periods. Perhaps the most striking result obtained is that the process of depolarization

(stimulated by surface anchoring interactions) leads to the disappearance of helices of appropriately large periods. Although the model presented here concerns LC systems with smectic layers oriented perpendicular to surfaces of thin confining cells, one can expect that the results derived by using the model will turn out to be helpful for investigating possible mechanisms to form complex helical structures occurring in other confining geometries, for which the orientation of molecules within smectic layers is distinctly inhomogeneous. In particular, this may concern LCs in the freestanding film geometry.

ACKNOWLEDGMENTS

This work was supported by the funds for science in years 2010–2013 as a research project.

[1] H. Takezoe, E. Gorecka, and M. Čepič, Rev. Mod. Phys. **82**, 897 (2010).
[2] Z. Q. Liu, B. K. McCoy, S. T. Wang, R. Pindak, W. Caliebe, P. Barois, P. Fernandes, H. T. Nguyen, C. S. Hsu, S. Wang, and C. C. Huang, Phys. Rev. Lett. **99**, 077802 (2007).
[3] S. Wang, L.-D. Pan, R. Pindak, Z. Q. Liu, H. T. Nguyen, and C. C. Huang, Phys. Rev. Lett. **104**, 027801 (2010).
[4] H. Orihara and Y. Ishibashi, Jpn. J. Appl. Phys. **29**, L115 (1990).
[5] H. Sun, H. Orihara, and Y. Ishibashi, J. Phys. Soc. Jpn. **62**, 2706 (1993).
[6] V. L. Lorman, A. A. Bulbitch, and P. Toledano, Phys. Rev. E **49**, 1367 (1994).
[7] M. Čepič and B. Žekš, Mol. Cryst. Liq. Cryst. **263**, 61 (1995).
[8] M. Škarabot, M. Čepič, B. Žekš, R. Blinc, G. Heppke, A. V. Kityk, and I. Muševič, Phys. Rev. E **58**, 575 (1998).
[9] A. Roy and N. V. Madhusudana, Eur. Phys. J. E **1**, 319 (2000).
[10] M. Čepič and B. Žekš, Phys. Rev. Lett. **87**, 085501 (2001).
[11] D. A. Olson, X. F. Han, A. Cady, and C. C. Huang, Phys. Rev. E **66**, 021702 (2002).
[12] R. Douali, C. Legrand, V. Laux, N. Isaert, G. Joly, and H. T. Nguyen, Phys. Rev. E **69**, 031709 (2004).
[13] A. V. Emelyanenko, Eur. Phys. J. E **28**, 441 (2009).
[14] A. V. Emelyanenko and M. A. Osipov, Phys. Rev. E **68**, 051703 (2003).
[15] A. V. Emelyanenko and M. A. Osipov, Ferroelectrics **309**, 13 (2004).
[16] M. B. Hamaneh and P. L. Taylor, Phys. Rev. E **75**, 011703 (2007).
[17] A. V. Emelyanenko, Phys. Rev. E **82**, 031710 (2010).
[18] M. A. Handschy, N. A. Clark, and S. T. Lagerwall, Phys. Rev. Lett. **51**, 471 (1983).
[19] J. E. Maclennan, N. A. Clark, M. A. Handschy, and M. R. Meadows, Liq. Cryst. **7**, 753 (1990).
[20] W. Jeżewski, W. Kuczyński, and J. Hoffmann, Phys. Rev. E **73**, 061702 (2006).
[21] P. V. Dolganov, Y. Suzuki, and A. Fukuda, Phys. Rev. E **65**, 031702 (2002); L. D. Pan and C. C. Huang, *ibid*. **83**, 060702(R) (2011).
[22] W. Jeżewski, W. Kuczyński, D. Dardas, K. Nowicka, and J. Hoffmann, Soft Matter **6**, 2786 (2010).
[23] S. T. Lagerwall, in *Ferroelectric and Antiferroelectric Liquid Crystals* (Wiley-VCH, Weinheim, 1999), p. 319.
[24] P. Rudquist, J. P. F. Lagerwall, M. Buivydas, F. Gouda, S. T. Lagerwall, N. A. Clark, J. E. Maclennan, R. Shao, D. A. Coleman, S. Bardon, T. Bellini, D. R. Link, G. Natale, M. A. Glaser, D. M. Walba, M. D. Wand, and X.-H. Chen, J. Mater. Chem. **9**, 1257 (1999).
[25] W. Jeżewski, W. Kuczyński, and J. Hoffmann, Phys. Rev. E **83**, 042701 (2011).
[26] I. Muševič and M. Škarabot, Phys. Rev. E **64**, 051706 (2001).
[27] F. Gouda, K. Skarp, G. Andersson, H. Kresse, and S. T. Lagerwall, Jpn. J. Appl. Phys. **28**, 1887 (1989).
[28] D. Dardas, W. Kuczyński, J. Hoffmann, and W. Jeżewski, Meas. Sci. Technol. **22**, 085707 (2011).
[29] K. Kondo, H. Takezoe, A. Fukuda, and E. Kuze, Jpn. J. Appl. Phys. **21**, 224 (1982).
[30] W. Kuczyński, Phys. Rev. E **81**, 021708 (2010).
[31] B. Kutnjak-Urbanc and B. Žekš, Phys. Rev. E **48**, 455 (1993).